applied sciences

MDPI

Article

On the Rheological Memory and Cumulative Damage of Thermoplastic Starch Biodegradable Films Reinforced with Nanoclay

Eleni Kazantzi †, Melpomeni Christou †, Theofilos Frangopoulos, Anna Marinopoulou, Athanasios Goulas, Dimitrios Petridis * and Vassilis Karageorgiou *

Department of Food Science and Technology, International Hellenic University, P.O. Box 141, 57400 Thessaloniki, Greece; elenikazantzh@gmail.com (E.K.); menh782@gmail.com (M.C.); thfrangopoulos@gmail.com (T.F.); amarinop@ihu.gr (A.M.); agoulas@ihu.gr (A.G.)

* Correspondence: petridis@ihu.gr (D.P.); vkarageorgiou@ihu.gr (V.K.); Tel.: +30-23-1001-3917 (D.P.); +30-23-1001-3906 (V.K.)

† These authors contributed equally to this work.

Abstract

Although the strain hardening phenomenon has been studied in different types of materials, there are only a few such reports regarding flexible food packaging. To address this issue, nanoclay-reinforced and control starch-based films were subjected to sequential and weekly tension and the rheological index, defined as the ratio of the tensile strength observed under weekly to that under consecutive elongation, was measured. The results showed that the values of the rheological index were >1, implying a strain hardening effect that was more notable when nanoclay was added and when the stress duration was increased. Additionally, a cumulative damage test was conducted, involving the gradual increase of two factors in each step: the percentage of the elongation level and the duration of each step. The data were fitted to a linear model, describing the correlation between the ln failure time (μ) and the tensile strength (X), $\mu = 6.021 - 0.478\,X$. This model enabled the prediction of the failure probability and the hazard rate of the films that were studied. In addition, from the survival of the units in the initial steps of the cumulative damage experiment, it can be hypothesized that the elongation of the units under low stress levels, for prolonged periods of time, exhibits rheological memory properties, which leads to an increase in their mechanical strength.

Keywords: starch biodegradable films; nanoclay; rheological memory; strain hardening; cumulative

check for updates

Academic Editors: Rafael G. Araújo and Maricarmen Iñiguez-Moreno

Received: 10 September 2025
Revised: 15 October 2025
Accepted: 17 October 2025
Published: 17 October 2025

Citation: Kazantzi, E.; Christou, M.; Frangopoulos, T.; Marinopoulou, A.; Goulas, A.; Petridis, D.; Karageorgiou, V. On the Rheological Memory and Cumulative Damage of Thermoplastic Starch Biodegradable Films Reinforced with Nanoclay. *Appl. Sci.* **2025**, *15*, 11166. https://doi.org/10.3390/app152011166

Copyright: © 2025 by the authors. Licensee MDPI, Basel, Switzerland. This article is an open access article distributed under the terms and conditions of the Creative Commons Attribution (CC BY) license (https://creativecommons.org/licenses/by/4.0/).

1. Introduction

Packaging is an important factor that ensures the protection and preservation of the integrity of a product. It plays a key role in product handling, transportation and distribution, and has a profound influence on the consumer's decision to buy. The value of food packaging, in particular, is considered of major importance because it contributes to the well-being and health of the consumers, since it acts as a barrier against the external contaminants such as micro-organisms, dust, gases, and light. The most popular and widely used food packaging materials are made of petrochemical polymers due to their high resistance to degradation, low cost, and excellent mechanical and optical properties [1,2].

However, environmental safety is a key area of concern for the widespread use of plastics, as it is estimated that over 300 million tons of plastic waste is generated globally

each year, much of which comes from single-use food packaging [2]. The extensive use of synthetic plastics, and consequently, the risk of potential environmental contamination that exists throughout the synthetic polymer life cycle, from the synthesis of the monomer to landfill deposition and recycling, necessitates the development of alternative products such as biopolymers [3].

A sustainable alternative to the problems associated with conventional food packaging, are the biodegradable food packaging materials made from renewable biological resources. Their limitations as packaging materials are related to some of their characteristics, such as limited barrier properties, susceptibility to thermal degradation, low mechanical strength, and high cost. The implementation of techniques such as lamination, blending, reinforcement with nanomaterials, and multilayer composite structures has broadened the applicability of biopolymers in various food products [4].

Nanomaterials have gained a growing interest in recent years [5] due to the properties they can offer in food packaging applications, as they enhance mechanical and thermal properties and exhibit resistance to gas diffusion, being toxicologically safe and biodegradable [6]. Thus, the use of reinforcing materials such as nanoclay-based nanostructures, metal and their oxides, biomass-based nanostructures, carbon-based nanomaterials and so on, has been applied to both synthetic and biobased food packaging materials in order to enhance the reliability of food packaging [7].

To ensure the functionality of the nanocomposite packaging, it is essential to determine its lifetime under various stresses that adequately simulate the actual conditions to which it will be exposed during use. For the prediction of the material's lifetime, the concepts of rheological memory and cumulative damage have been introduced. The majority of published studies that examine the effects of strain and the number of stress cycles on the properties of rheological memory (strain hardening) primarily focus on metal materials [8,9], followed by synthetic polymers [10,11]. Strain hardening in flexible food packaging films has been investigated in only a limited number of cases, including studies on polypropylene blends [12], poly (lactic acid) [13], and poly (lactic acid) and polyamide 11 blend films [14]; therefore, further research on the structural characteristics related to fatigue loads and their effect on the rheological memory of biodegradable packaging materials is needed.

Cumulative damage models study the deterioration of unit performance as a result of their stress exposure due to the action of various stress-inducing factors, with a gradual increase in intensity in recording the action at arbitrary timepoints. A cumulative damage experiment, also known as a varying-stress experiment, is a type of accelerated life test in which the stress factor levels can increase over time. A typical step–stress experiment consists of multiple test units, where each unit is subjected to an initial level of stress, and this level is gradually increased during the experiment, while the failure time is recorded as the response variable. Cumulative damage experiments have not been conducted in packaging films; examples of other cases are polysilicon films for microelectromechanical systems (MEMS) resonators [15], copper films [16] and thin films in plastic-integrated circuits [17]. The accelerating factors of these studies include temperature [17], loading [15,16], and voltage [18]. However, in all cases, the authors developed complex mathematical models and algorithms based on the damage equalization method [18], continuum damage mechanics (CDM) theory [15], and a general reliability model constituted by a two-parameter Weibull distribution and a differential equation [17].

The aim of this study was to evaluate the influence of rheological memory when applying fatigue tests to polymeric material. Specifically, the rheological memory of nanocomposites, thermoplastic, starch-based biopolymers, and its influence on their lifetime was investigated. Additionally, as the cyclic stress concept cannot approach the actual conditions to which the material is exposed accurately enough, the behavior of the

material was tested when subjected to progressively increasing elongation levels. The accelerated life tests can more accurately estimate the factors with which the material under test interacts, since the stress to which it is subjected has a cumulative nature due to stress accumulation in the material. Therefore, in the present work, the accelerated staggered stressing is applied for the first time in packaging films using the elongation as a stress factor and a simple statistical method for the prediction of failure life is proposed.

2. Materials and Methods

2.1. Materials

Lentil (*Lens culinaris*) starch was extracted as described elsewhere [19]. Glycerol of 99% purity was acquired from Carlo Erba Reagents (Cornaredo, Italy) and montmorillonite (MMT) (bis(hydrogenated tallow alkyl)dimethyl, salt with bentonite, <80 nm APS, 99% purity, 1.98 g/cm^3 density, <3% moisture) was obtained from Nanocel LG (Punjab, India).

2.2. Experimental Design

2.2.1. Rheological Memory

In order to assess the impact of rheological memory on the lifetime of the experimental film units, nanoclay-reinforced starch films and control films were fabricated. The experimental design contained various combinations of constant elongation levels and application times, representing different treatments (Table 1). Ten films from each treatment were divided into two separate categories depending on the application of stress cycles. Specifically, 5 units were subjected to immediately repeated stress cycles, while the other 5 units underwent one stress cycle per week, until the films from both categories broke. The difference between the units that underwent consecutive and weekly experimental trials lies in the time frame between stress cycles. In the consecutive trials, the time frame between each cycle was zero, whereas in the weekly trials, it was one week.

Table 1. Experimental design of consecutive and weekly experimental treatments.

Sample Name	Nanoclay Reinforcement	Elongation Level (%)	Application Time (min)
5%-2′ control	no	5	2
5%-2′ MMT	yes		
5%-5′ control	no	5	5
5%-5′ MMT	yes		
7%-2′ control	no	7	2
7%-2′ MMT	Yes		

2.2.2. Cumulative Damage Test

This experimental design consisted of seven steps, each of which was a combination of a stepwise elongation rate and different times of stress application. Ten units were used for each stress pattern and were subjected to seven steps of progressively increasing elongation, 3, 7, 10, 12, 15, 17, and 20%, following an analogous design experimented by Nelson (1990) [20]. In each stress pattern, the elongation levels of each step were the same, but the duration of the application differed, except for the first three steps, where the stress/time combinations remained the same for all stress patterns (Table 2). The reasoning for choosing the same stress/time combinations in the first three steps of each stress pattern was that, according to preliminary experiments, these stress conditions would result in no broken units. The failure time in cumulative mode of the units and their tensile strength at break at each step were recorded.

Table 2. Layout of the cumulative damage experimental design.

Stress Pattern	Step	Elongation Level (%)	Elongation Duration (min)
1	1	3	5
	2	7	5
	3	10	5
	4	12	10
	5	15	10
	6	17	10
	7	20	10
2	1	3	5
	2	7	5
	3	10	5
	4	12	20
	5	15	20
	6	17	20
	7	20	20
3	1	3	5
	2	7	5
	3	10	5
	4	12	40
	5	15	40
	6	17	40
	7	20	40

2.3. Film Preparation

Since nanoclay presents low dispersibility in aqueous dispersions, for the preparation of the nanoclay-reinforced films, nanoclay aqueous dispersions were prepared by stirring at 200 rpm for 24 h and sonicating at 15,000 kHz for 15 min. This process was carried out in order to ensure the formation of a homogeneous dispersion. An aqueous thermoplastic starch dispersion was formed by continuously stirring starch (6.5% *w*/*w*) and glycerol (35 or 50% *w*/*w* based on dry starch) in distilled water at 80 °C in a water bath for 40 min. During this process, the phenomenon of starch gelatinization took place, since when the starch is subjected to its gelatinization temperature in excess water, its crystalline and structural organization are permanently disturbed. After the gelatinization of starch, the temperature was increased to 90 °C, followed by the addition of the MMT dispersion (so that the final concentration of MMT was 10.5% *w*/*w* based on dry starch) and heating under continuous stirring for 15 min. This process enabled the efficient intercalation of starch polymer chains in between nanosilicate sheets. Furthermore, a reduction in viscosity was achieved, which facilitated the application of the mixture to the drying trays. The presence of MMT enhances the mechanical properties of the material, while glycerol enhances its elasticity, properties that are crucial for the rheological memory and cumulative damage experiments. Control films were prepared following the same procedure without the addition of MMT, and therefore without increasing the temperature after the completion of the gelatinization process. Finally, the dispersion was placed in 18 cm × 11 cm plexiglass trays and then dried at a temperature of 40 °C for 17 h in an air-circulating oven. Upon completion of drying, the films were removed from the trays and left for a week in ambient conditions (25 °C and ~60% RH) to balance the moisture content and increase their elasticity. The composition of films for each test, as determined from preliminary experiments, is shown in Table 3.

Table 3. Composition of films for the rheological memory and cumulative damage experiments.

Experiment		Composition (Based on Dry Starch) Glycerol	MMT
Rheological memory	Nanoclay-reinforced films	35%	10.5%
	Control films		-
Cumulative damage		50%	10.5%

2.4. Tensile Tests

The mechanical properties of each experimental film unit for both tests were evaluated using tensile tests that determined the correlation between the applied stress and the survival of the units. The tensile test was conducted at 25 °C and ~60% RH. The tensile properties of the film samples were measured according to the ASTM D882-10 [21] standard test method. For each test, film specimens were cut with a lancet at 120 mm length and 15 mm width and the thickness of each sample was measured using a digital electronic caliper (TESA, Brown & Sharpe Instruments, Grand Rapids, MI, USA) (a total of 12 measurements were taken from each film). The functional part of the film specimens was 100 mm long and the remaining 20 mm were the non-functional areas, i.e., the surface enclosed between the grips of the texture analyzer (TA.XT Plus, Stable Micro Systems, Godalming, UK), when securing the film specimen. Each sample was placed with the instrument grips in full extension. The experiments were carried out at an ambient temperature (23 °C), with a crosshead speed (rate of grip separation) of 50 mm min^{-1}. The tensile strength was calculated by dividing the maximum applied force recorded for the film unit under test by the cross-sectional area (product of the thickness times the width) of the unit.

2.5. Statistical Analysis

2.5.1. Rheological Memory

To compare the responses of the experimental units under weekly and consecutive stresses, an empirical index of rheological memory was utilized. This index quantifies the material's rheological memory response by evaluating the ratio of the tensile strength observed under weekly stretching to that under consecutive elongation. Mathematically, the index is defined as the ratio of the tensile strength observed under weekly stretching to that under consecutive elongation. The term σ_{weekly} represents the tensile strength of the weekly elongation, while the term $\sigma_{consecutive}$ refers to the tensile strength of the consecutive elongation.

$$rheological\ memory\ index = \frac{\sigma_{weekly}}{\sigma_{consecutive}} \quad (1)$$

2.5.2. Cumulative Damage Test

The statistical analysis of this experiment is known as reliability and survival analysis, and is used for the description of the lifetime of various test units; therefore, life distributions were utilized. The statistical process and representation of the results from the accelerated life test was performed with specific diagrams. Specifically, using the JMP 17.1 program (JMP, Cary, NC, USA), the following distributions and diagrams were constructed:

- The plot of events, which details the response of each studied experimental unit for a specific time record. Notably, because reliability experiments are conducted over a finite duration, any unit that has not failed by the end of the study is considered right censored, as its actual failure time is only known to exceed the study period.
- The cumulative damage diagram, which plots the tensile strength versus failure time.
- The F(t) distribution diagram, which represents the cumulative probability of failure as a function of the lifetime of the units.

- The quantile plot of time, which describes the hold time as a function of the cumulative probability.
- The hazard plot h(t), which illustrates the hazard rate as a function of the hold time.

The cumulative damage experiment was analyzed exclusively using the JMP 17.1 statistical procedure. This comprehensive analysis enabled a detailed evaluation of the experimental data, providing insights into the behavior and failure characteristics of the studied units.

3. Results and Discussion

3.1. Rheological Memory

The thickness of the films that were subjected to the tensile test in the rheological memory experiment was 0.172 ± 0.032 mm for the control films and 0.231 ± 0.051 mm for the nanoclay-reinforced films. Nanoclay-reinforced films were thicker due to the higher amount of solids present in these films (10.5% MMT based on dry starch). The moisture of the control films was 15.65 ± 0.58% and was not significantly different than that of nanoclay-reinforced films, which was 14.38 ± 0.82%.

The rheological memory indices of the different treatments are presented in Figure 1, while representative tensile strength–strain curves are presented in Figure 2. In all cases (the only exception being the non-reinforced sample subjected to 7% elongation for 2 min), the rheological memory indices were higher than 1, signifying that the tensile strength of the weekly elongation was higher than the tensile strength of the consecutive elongation. This result was more notable in the case of nanoclay reinforcement, showing that the presence of nanoclay had a significant effect on strain hardening; even in the case of samples subjected to 5% elongation for 2 min, where the rheological memory index of the nanoclay-reinforced sample was lower than the rheological memory index of the non-reinforced sample, the values were very close. The increase in the stress duration (from 2 min to 5 min for 5% elongation) resulted in higher rheological memory indices, particularly in the case of the nanoclay-reinforced sample. No specific effect could be observed regarding the effect of increasing the stress level (from 5% to 7% elongation for 2 min), since in the case of the non-reinforced sample, there was a reduction, but in the case of the nanoclay-reinforced sample, there was a slight increase.

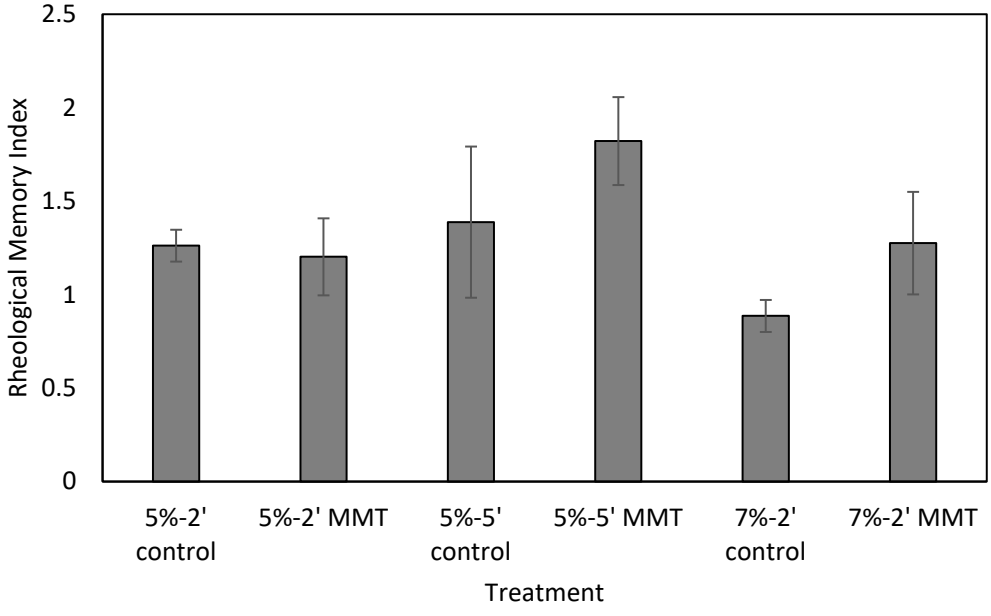

Figure 1. Distribution of mean rheological memory indices among the six treatments. Vertical bars denote standard errors of five replicates.

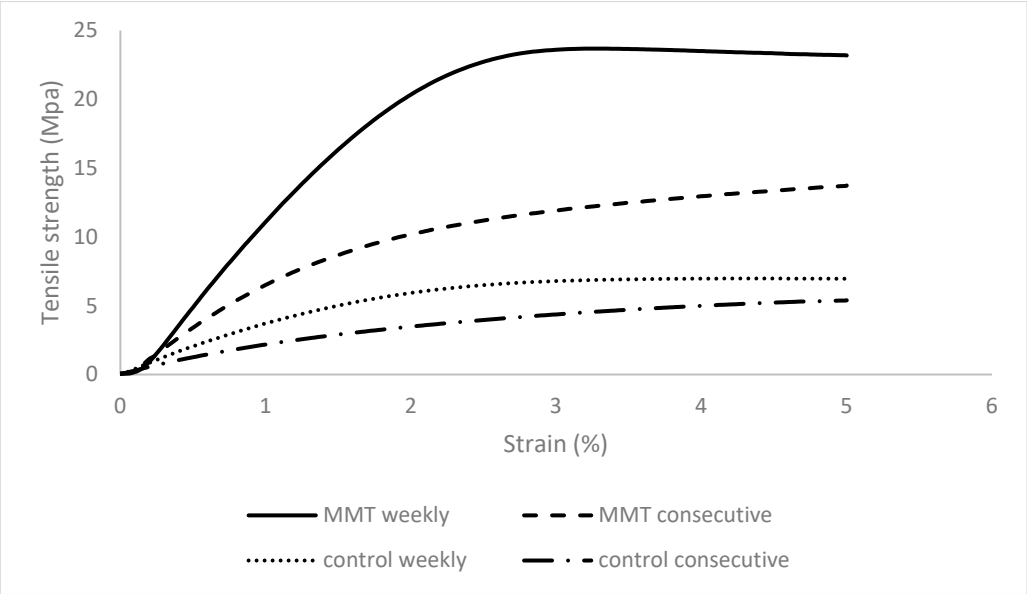

Figure 2. Representative tensile strength–strain curves for the 5%-5′ protocol.

The strain hardening phenomenon is due to the rheological properties developed during the stress tests. From the findings of the experimental processes, it can be concluded that the increase in the stress duration had a positive effect on the strain hardening phenomenon, as it gave a greater period of time for the nanoclay and starch molecules to come into contact through tensile force and form bonds between them. When the nanoclay particles were incorporated into the thermoplastic starch matrix, the formation of additional bonds between the nanoclay particles and the thermoplastic starch (gelatinized starch and glycerol) components took place. These bonds created cross-linking nodes (junction zones) that contributed to the material's tensile strength. During elongation, the cross-linking nodes moved closer, resulting in the formation of numerous new secondary bonds. While these secondary bonds were not enthalpic and exhibited low individual strength, their large quantity compensated for their weakness. A portion of these bonds persisted even after the initial elongations and multiplied during subsequent stretching, further increasing the tensile strength. This behavior caused a gradual improvement in the system's time constant, which enhanced the material's tensile strength. The observation that the increase in the stress level did not affect the rheological memory index could probably be associated with the fact that the increased stress level surpassed a critical level and caused damage to the film matrix that was higher than the bonds that were created between the starch chains and the nanoclay.

The number of cycles that each treatment underwent until break is presented in Figure 3. In general, samples that underwent consecutive elongation lasted for more cycles until break compared to the samples that underwent weekly elongation. There were only two exceptions: the nanoclay-reinforced sample subjected to 5% elongation for 2 min, where the number of cycles was equal for both the consecutive and weekly stress regimes; and the nanoclay-reinforced sample subjected to 5% elongation for 5 min, where the number of cycles was higher for the weekly stress regime. This result is in good agreement with the rheological memory index result, because, since the rheological memory index is higher than 1, samples that underwent the weekly stress regime became tougher than samples that underwent the consecutive stress regime; thus, they became less flexible, and therefore, lasted for fewer cycles until break. The difference between the number of cycles of the consecutive and weekly stress regimes was less notable for nanoclay-reinforced samples, indicating that the presence of nanoclay plays a role in the strain hardening phenomenon.

Both the increase in the stress duration (from 2 min to 5 min for 5% elongation) and the increase in the stress level (from 5% to 7% elongation for 2 min) resulted in a reduction in the number of cycles until break. This is expected because both increases contributed to the strain hardening phenomenon, resulting in tougher films, which were less flexible and withstood a lower number of cycles until break.

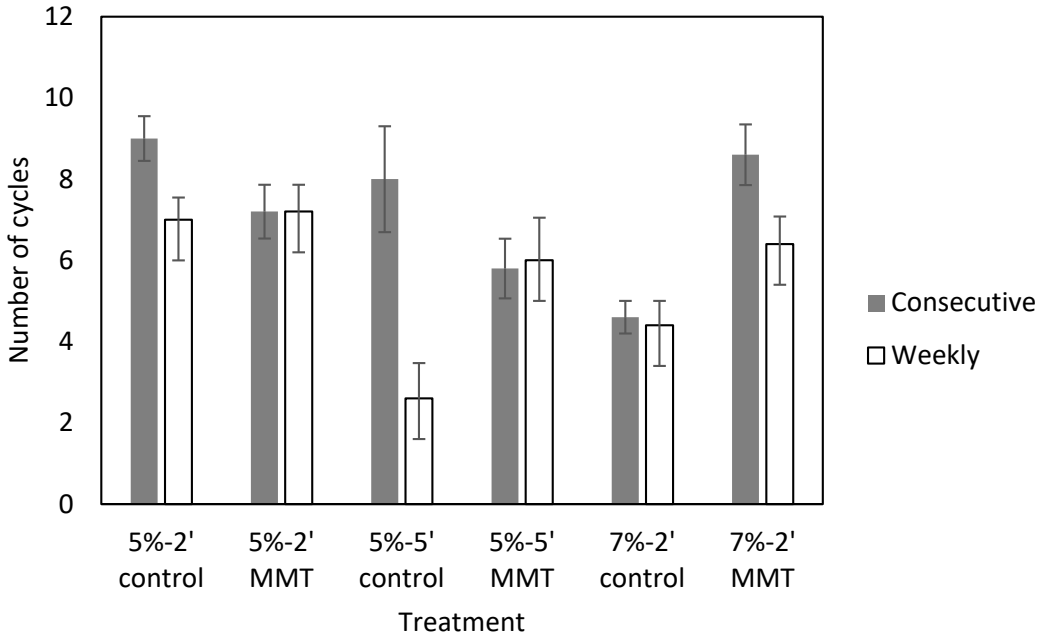

Figure 3. Distribution of mean number of cycles until break for the weekly and consecutive elongation. Vertical bars denote standard errors of five replicates.

The aforementioned results indicate that increasing the stress either in the form of stress duration or in the form of stress level resulted in a reduction in the failure life of the experimental units. Previous research on the effect of stress increase to the failure life was mainly applied to metallic materials. Therefore, due to the differing nature of the materials considered, a direct comparison of the results is not feasible. However, it is possible to evaluate the effect of the tests in the experimental units with those of other studies, as the mechanisms involved are common. The results of this study agree with the findings of Zhu et al. (2022) [22], who performed tensile tests on AA6082 anodized alloy sheets. Specifically, they used two groups for the stress experiments with tensile strength values of 150 MPa and 170 MPa. When the tensile strength was 150 MPa, the specimen fractured when the number of cycles was 2.1×10^5, while at 170 MPa, the specimen fractured when the number of cycles was 1.4×10^5 (Zhu et al., 2022) [22]. Furthermore, based on the theory of continuous damage mechanics, Liu et al. (2021) [23] developed a fatigue cumulative damage model which predicted that increasing the stress has a negative effect on the failure life of the material. More specifically, they simulated different levels of tensile strength as a stress factor for metal alloys exhibiting shape memory alloy (SMA) properties. When the tensile strength level was 500 MPa, the experimental unit was predicted to withstand 2128 cycles, whereas when the level was increased to 600 MPa, the fatigue life decreased to 250 cycles [23].

Although strain hardening has not been studied in starch films, it has been studied in other starch forms. Strain hardening is important in breadmaking, since it affects the quality of the produced bread and is attributed to the entanglement coupling of large glutenin molecules, the formation of interchain β sheets or the finite extensibility of elastically effective network chains [24]; the addition of high amylose wheat starch to wheat flour dough has been shown to enhance this phenomenon [25]. Milky and dough starch pastes

showed a minor degree of strain hardening, but this effect was not observed in mature starch pastes [26]. The strain hardening behavior was observed in the urea–formamide-plasticized, but not in the glycerol-plasticized thermoplastic starch melts [27]. Finally, the appearance of the strain hardening phenomenon in wheat starch–oleic acid gel systems was attributed to the formation of complexes and the formation of the V-type crystalline structure [28].

Strain hardening phenomena in the field of biopolymers have been described in the literature and are shown in the present study, both in the presence of nanoclay and not. More specifically, it is shown that weekly tensile loads on starch films with or without nanoclay had higher stress values than consecutive loads, due to strain hardening phenomena that were generated through aging after stress application. The degrading effect of prolonged fatigue cycling tension of films on the mechanical attributes of films is well described in the literature [29]. The aging of PLA films caused a decrease in stress values, when tensile loads were applied after 45 or 90 days after manufacturing [30]. Moreover, the effect of different stress intensity and fatigue behavior was also investigated in PLA films tested at 3 and 30 Hz [31]. In this study, it was observed that increasing the stress intensity caused a notable decline in the number of cycles until failure, which was more pronounced in PLA films reinforced with 5% w/w nanoclay than control PLA films, particularly at low frequencies. In the present study, this was also found, and it is best described in Figure 3, where number of cycles until break was always higher at control films than films with nanoclay. Other stress types, like bending, water, and temperature, have been investigated in films. For example, the hydrolytic aging at different temperatures and time was investigated in PBAT films and it was found that aging had a lower impact on the mechanical attributes of PBAT films at lower temperatures [32]. Also, when different bending loads were applied to PLA–wood 3D-printed materials, it was found that, at higher bending loads, the lifetime of products was the lowest [33]. These findings are in agreement with the results of the present study, where increasing the stress from 2 to 7%, or the duration from 2 to 5 min, caused a significant reduction in the weekly cycles until break (Figure 3).

3.2. Cumulative Damage Test

The results of the cumulative damage test are shown in Table 4. The test consisted of graded levels of applied stress where the fatigue load of the units had a cumulative nature. From the experimental data, it is evident that, as the elongation level increased, the tensile strength also increased, with the exception of the sixth step of the experimental design, which presented a higher value than that of the seventh. In the third stress pattern, it was observed that the highest values occurred for the three initial steps; however, in the following steps, the response pattern that was recorded in the first two stress patterns was restored. This fact is probably due to random experimental error. In the first three steps, where the strain duration remained constant for each stress pattern, it was observed that the values of the tensile strength were similar. However, in the next four steps, as the stress duration increased from stress pattern 1 up to stress pattern 3, the values varied in each stress pattern. In particular, the maximum trends were observed in the first pattern (shortest stress duration) and the minimum in the third (longest stress duration). Therefore, an increase in the stress duration caused a decrease in the tensile strength response.

Table 4. Cumulative damage test results. The term "censored" refers to the experimental units that have survived a stress step and whose failure time is not known (the values recorded in the failure time for these experimental units refer to the duration of the step), while the term "failed" refers to the experimental units that did not pass the applied stress level.

Stress Pattern	Step	Stress Duration (min)	Elongation %	Failure Time (min)	Number of Censored/Failed Films	Tensile Strength (MPa)
1	1	5	3	5	10/0	2.9
	2	5	7	10	10/0	3.19
	3	5	10	15	10/0	3.16
	4	10	12	15.86	8/2	5.28
	5	10	15	27.09	6/2	5.54
	6	10	17	37.17	1/5	6.21
	7	10	20	47.16	0/1	6.09
2	1	5	3	5	10/0	2.94
	2	5	7	10	10/0	2.62
	3	5	10	15	10/0	2.78
	4	20	12	19.97	7/3	3.12
	5	20	15	38.54	4/3	4.95
	6	20	17	64.14	1/3	5.2
	7	20	20	75.64	0/1	4.38
3	1	5	3	5	10/0	4.16
	2	5	7	10	10/0	5.03
	3	5	10	15	10/0	4.04
	4	40	12	45.69	6/4	2.94
	5	40	15	67.61	2/4	3.54
	6	40	17	104.17	1/1	3.89
	7	40	20	106.2	0/1	3.6

All the experimental units, as shown in Figure 4, endured the initial three steps of stress (3, 7, and 10% elongation), and as a result, they survived. At the next four steps (12, 15, 17, and 20% elongation) all experimental units ruptured, with the shortest failure times corresponding to the experimental units of the first stress pattern and the longest occurring in experimental units of the third. This fact is due to the increase in the duration of the applied stress at each step beyond the initial three stress, which caused a decrease in the failure time of the films. Increasing the duration of the applied stress caused an increase in the failure time of the films. This can be explained by the fact that tension aligned and brought the starch chains closer, creating new secondary bonds between them and this phenomenon was accentuated as the duration of the applied stress increased; therefore, strain hardening during tension of starch films was observed in the cumulative damage experiment as well. Previous research on the application of strain gauge as a method of predicting the lifetime of materials has mainly been applied to metal materials. Therefore, due to the different nature of the materials under consideration (the metallic bond is a primary bond and metals are crystalline materials), a direct comparison of the results is not possible. However, the effect of the tests on the experimental units can be evaluated with those of other studies since the mechanisms involved are common. Thus, it appears that the results of this study converge with the results of Kim et al. (2017) [34] on the cyclic creep properties of Grade 91 steel, which demonstrated that the failure time increased as the stress ratio increased [34].

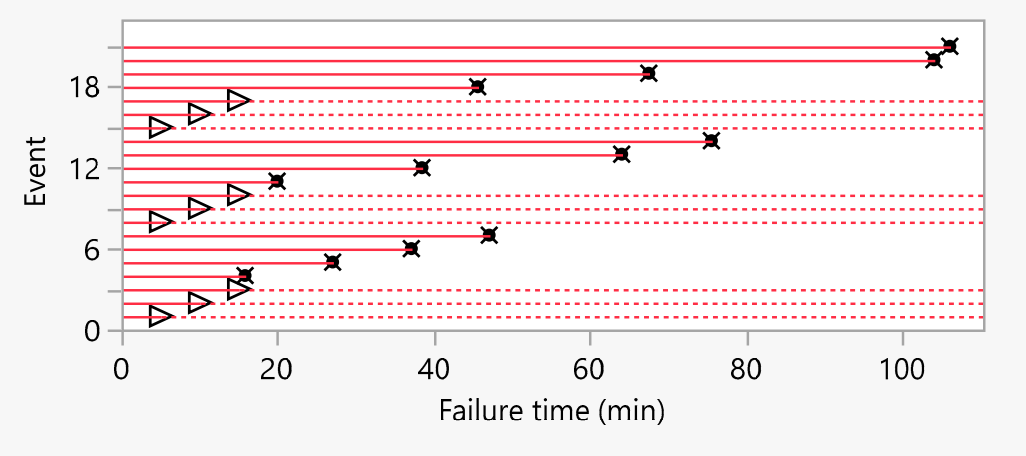

Figure 4. Event plot of experimental units vs. failure time, where —x stands for specific failure time (uncensored unit), and —▷----- stands for censored elements in which the failure time is impossible to record.

From Figure 5 it can be observed that the changes in the treatments corresponding to stress patterns 1 and 2 (10 and 20 min, respectively), followed a similar response pattern of tensile strength reduction with failure time. Regarding stress pattern 3, the highest tensile strength values were recorded at the initial three steps (3, 7, and 10% elongation). This discrepancy was ascribed to a random experimental error in the structure of the material during the film preparation process and is the main cause of the heterogeneity in the initial steps of the specific stress pattern.

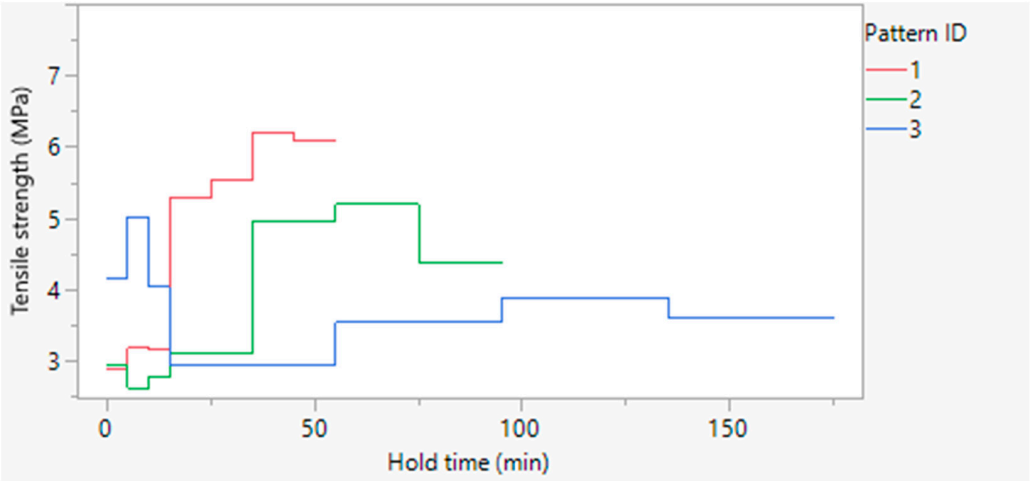

Figure 5. Cumulative damage diagram of tensile strength by hold time according to the three increasing stress patterns of films.

The results of the tensile strength parameterization are shown in Table 5. The effect of tensile strength on the experimental units was studied with the application of the linear regression model. The linear model was characterized by three parameters, the slope b_1, the height of the line b_0 and the index β which is the shape parameter of the Weibull distribution. Shape coefficients greater than 2 describe hazard profiles with concave curves of hazard rate becoming more opening with increasing values. Coefficients lower than 1 describe a 'weakest link' process, which is better established by the theory of the smallest extreme values distribution (SEV). The assessment of the goodness of fit of the data in the model was determined by the -2LL (log likelihood) value, where the smaller the value, the better the fit of the data. In addition, the selection of the most appropriate distribution was

determined by the value of the information criteria AICc and BIC (Akaike and Bayesian information criteria, respectively), where a good fit of the data requires small values of these indices. According to the data, the Weibull distribution proved to be the best fit for this model, as it exhibits the smallest values in AICc and BIC coefficients. The equation of the resulting linear model, which describes the correlation between the ln failure time (μ) and the tensile strength (X), is

$$\mu = 6.021 - 0.478\,X \quad (2)$$

Table 5. Parameterization of tensile strength. The term -2LL expresses the log likelihood, N the number of observations and the AICc and BIC values denote the Akaike and Bayesian information criteria, respectively.

Distribution	-2LL	N	AICc	BIC
Weibull	107.12	3	114.37	116.51
Lognormal	109.96	3	117.20	119.35
Loglogistic	110.38	3	117.65	119.79
Exponential	113.69	2	118.29	119.97
Frechet	113.48	3	120.75	122.89
Parameter	**Value**	**SE**	**−95%**	**+95%**
b_0	6.021	0.791	4.470	7.571
b_1	−0.478	0.183	−0.837	−0.117
β	2.060	0.497	1.398	3.914

The negative sign of the coefficient b_1 shows that, an increase in the tensile strength by 1 MPa results in a reduction in the ln of failure time by 0.478 units (this means that the failure time decreases by 1.613 times). For 95% significance limits, the shape of its curve was β = 2.060, which corresponds to a linear increase in the hazard rate h(t) (Rayleigh distribution). According to these data, it is safe to conclude that the failure rate increased continually throughout the life of the films.

In Figure 6 it becomes apparent that, as the applied stress increases, the failure rate of the units intensifies. These results agree with the findings of Lv et al. (2014) [35], who reported that the creep lifetime of polypropylene/clay nanocomposites decreased, as the creep stress levels increased [35]. When the hold time is set to 50 min, the tensile strength is equal to 4.415 MPa and the probability of failure is 63.26%.

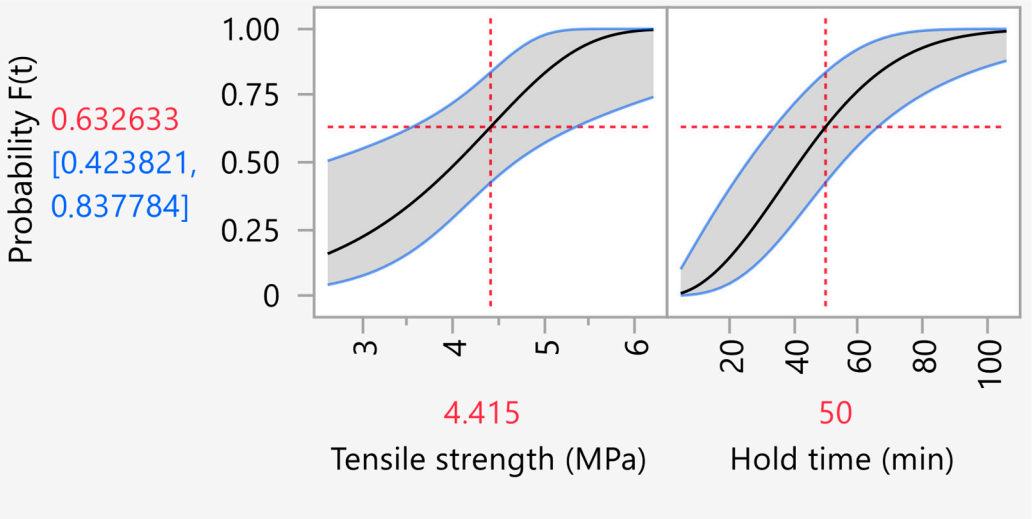

Figure 6. Cumulative profile of probability distribution vs. tensile strength and hold time of films.

As shown in Figure 7, increasing the hold time at which the unit is subjected to stress, caused a decrease at the tensile strength, and therefore, an increase in the probability of failure. A 50% probability of failure of the units is reached when the tensile strength is 4.415 MPa for a hold time of 41.8 min.

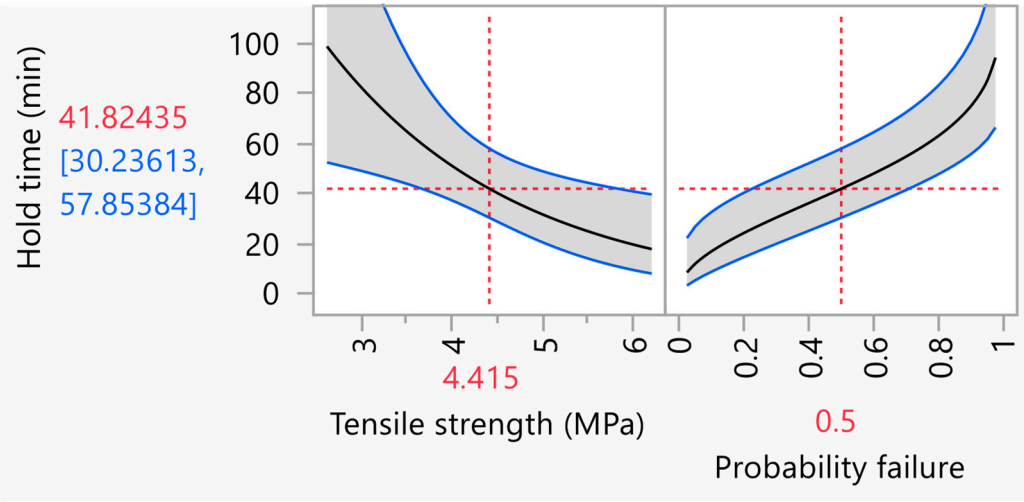

Figure 7. Quantile profile of hold time vs. tensile strength and probability failure of films.

In Figure 8, an upward trend in the hazard rate is observed, which demonstrates the failure of the experimental units as both the tensile strength and hold time increase. These results are verified by the parameter $\beta = 2.060$, obtained from the analysis of the Weibull model, which describes a linear variation in the risk rate. If the hold time of the experimental units is set to 50 min, the hazard rate tensile strength is 4.13% with a tensile strength of 4.415 MPa. If the applied tensile strength increases above the value of 4.415 MPa, the instantaneous hazard rate undergoes an exponential increase.

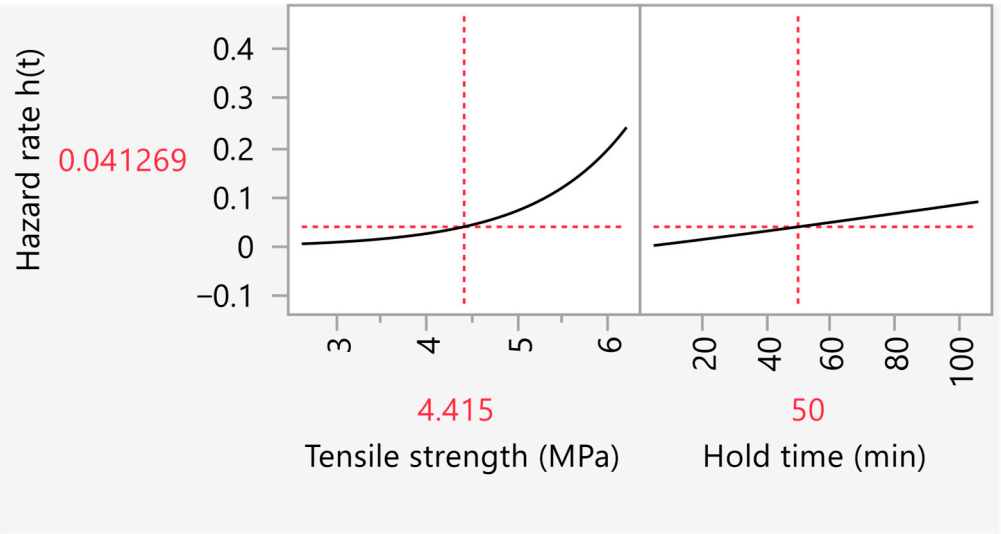

Figure 8. Hazard rate vs. tensile strength and hold time of films.

The reliability of the linear model is confirmed by the trend of the Cox–Snell residuals to closely surround the diagonal line (Figure 9a) and by the linear arrangement of the standardized residuals, since all points except for the first and the last one meet the requirements of normality (Figure 9b).

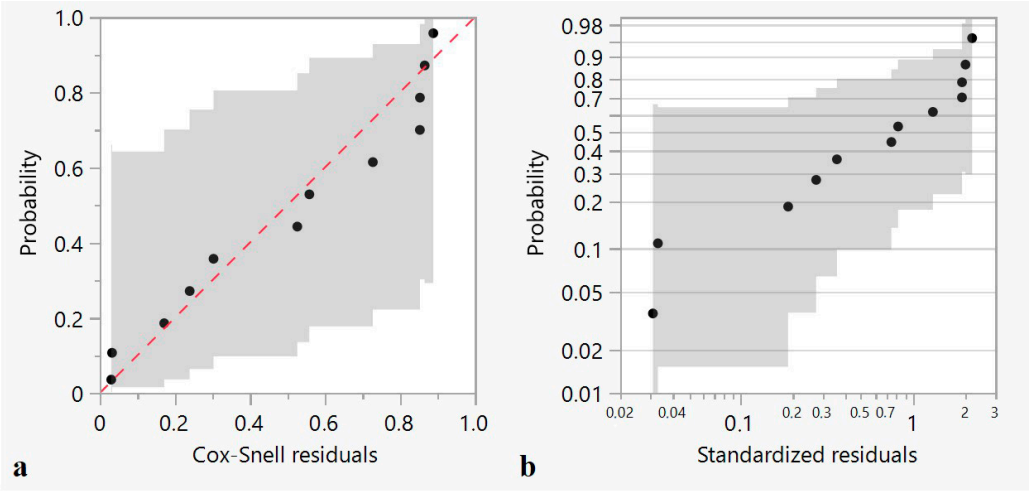

Figure 9. Probability graphs of normality using (**a**) Cox–Snell residuals and (**b**) standardized residuals.

Regarding the cumulative damage test, it was observed that an increase in the stress duration led to an extension of the lifetime of the experimental units. This behavior can be attributed to the dynamic formation of bonds during elongation. At lower elongation levels sustained over longer durations, there was sufficient time for stronger bonds to form. Specifically, the cross-linking nodes moved closer together, facilitating the creation of numerous new secondary bonds. This observation highlights the link between the rheological experiment and the cumulative test, as both demonstrate how the formation of bonds during elongation directly influences the mechanical performance and lifetime of the material during prolonged periods of stress.

4. Conclusions

The present study was carried out for the examination of the rheological memory that developed during the cyclic loading of nanoclay-reinforced starch films, which resulted in the occurrence of the strain hardening phenomenon. Furthermore, a model was developed that aimed to predict the mechanical behavior of the films under graded loading conditions, which had a cumulative damage profile and simulated the actual loading conditions to which the films will be subjected to during their usage with high accuracy. Both experiments demonstrated the beneficial effect of the increase in the applied stress duration on strain hardening; on the contrary, increasing the elongation level had a negative effect on the lifespan of films. Despite the variations due to the natural origin of the materials, this study paves the way for a deeper insight of the mechanical behavior of biodegradable starch film packaging.

The rheological memory index is a new concept, introduced in this study. There certain limitations regarding its application, since it only involves the ultimate tensile strength; therefore, to elucidate in depth the observed strain hardening phenomenon, additional concepts, such as elastic modulus, toughness, and nonlinear hardening slope from stress–strain curves, should be considered, while the Mullins effect and residual strain across cycles should be quantified. In order to substantiate secondary bond accumulation and junction zone evolution, essential experiments, such as X-ray diffraction, electron or atomic force microscopy, Fourier-transform infrared or Raman spectroscopy, and dynamic mechanical analysis could be conducted. These research directions will comprise part of the future work for the continuation of this study.

Author Contributions: Conceptualization, V.K. and D.P.; methodology, V.K. and D.P.; validation, V.K. and D.P.; formal analysis, D.P. and T.F.; investigation, E.K., M.C., T.F., A.M. and A.G.; resources, V.K.,

D.P. and A.G.; data curation, D.P. and T.F.; writing—original draft preparation, E.K., M.C., V.K. and D.P.; writing—review and editing, V.K. and D.P.; visualization, T.F., D.P. and V.K.; supervision, V.K. and D.P.; project administration, V.K.; funding acquisition, V.K. All authors have read and agreed to the published version of the manuscript.

Funding: The authors would like to acknowledge the financial support through the "StActBioFP" (#T6ΥΒΠ-00270) research program funded by the European Union—European Regional Development Fund and the Operational Program "Competitiveness, Entrepreneurship & Innovation" (EPAnEK) of the Partnership and Cooperation Agreement (NSRF) for the period 2014–2020.

Institutional Review Board Statement: Not applicable.

Informed Consent Statement: Not applicable.

Data Availability Statement: The original contributions presented in the study are included in the article, further inquiries can be directed to the corresponding authors.

Acknowledgments: We would like to thank Stylianos N. Raphaelides, Department of Food Science and Technology, International Hellenic University, for his helpful suggestions during the study and the preparation of the manuscript.

Conflicts of Interest: The authors declare no conflicts of interest.

References

1. Zannou, O.; Beşir, A.; Awad, N.M.H.; Oussou, K.F.; Odouaro, O.B.O.; Chabi, I.B.; Kpoclou, Y.E.; Kayodé, A.P.P.; Koca, I.; Selli, S. Chapter 4—Starch-based nanofibres for food packaging application. In *Starch Based Nanomaterials for Food Packaging*; Nayik, G.A., Hussain Dar, A., Eds.; Academic Press: Cambridge, MA, USA, 2024; pp. 83–102.
2. Chen, Y.; Awasthi, A.K.; Wei, F.; Tan, Q.; Li, J. Single-use plastics: Production, usage, disposal, and adverse impacts. *Sci. Total Environ.* **2021**, *752*, 141772. [CrossRef]
3. Awasthi, S.K.; Kumar, M.; Kumar, V.; Sarsaiya, S.; Anerao, P.; Ghosh, P.; Singh, L.; Liu, H.; Zhang, Z.; Awasthi, M.K. A comprehensive review on recent advancements in biodegradation and sustainable management of biopolymers. *Environ. Pollut.* **2022**, *307*, 119600. [CrossRef]
4. Cheng, J.; Gao, R.; Zhu, Y.; Lin, Q. Applications of biodegradable materials in food packaging: A review. *Alex. Eng. J.* **2024**, *91*, 70–83. [CrossRef]
5. Sharma, C.; Dhiman, R.; Rokana, N.; Panwar, H. Nanotechnology: An Untapped Resource for Food Packaging. *Front. Microbiol.* **2017**, *8*, 1735. [CrossRef] [PubMed]
6. Chaudhary, P.; Fatima, F.; Kumar, A. Relevance of Nanomaterials in Food Packaging and its Advanced Future Prospects. *J. Inorg. Organomet. Polym. Mater.* **2020**, *30*, 5180–5192. [CrossRef]
7. Bharathi, V.; Murugesan, P.; Moses, J.; Chinnaswamy, A. Recent Trends in Nanocomposite Packaging Materials. In *Reference Module in Food Science*; Elsevier: Amsterdam, The Netherlands, 2020.
8. Wang, J.; Misra, A. Strain hardening in nanolayered thin films. *Curr. Opin. Solid State Mater. Sci.* **2014**, *18*, 19–28. [CrossRef]
9. Tu, S.; Ren, X.; He, J.; Zhang, Z. Stress-strain curves of metallic materials and post-necking strain hardening characterization: A review. *Fatigue Fract. Eng. Mater. Struct.* **2020**, *43*, 3–19. [CrossRef]
10. Mukherji, D.; Abrams, C. Microvoid formation and strain hardening in highly cross-linked polymer networks. *Phys. Rev. E* **2008**, *78*, 050801. [CrossRef]
11. Münstedt, H. Various features of melt strain hardening of polymeric materials in uniaxial extension and their relation to molecular structure: Review of experimental results and their interpretation. *Rheol. Acta* **2023**, *62*, 333–363. [CrossRef]
12. Schubert, D.W.; Kaschta, J.; Seidl, S.; Kunzelmann, P. Binary and Ternary Blends of Polypropylene Types—Influence on the Homogeneity of Biaxial-Oriented Films. *Macromol. Symp.* **2016**, *365*, 87–94. [CrossRef]
13. Zhao, X.; Pelfrey, A.; Pellicciotti, A.; Koelling, K.; Vodovotz, Y. Synergistic effects of chain extenders and natural rubber on PLA thermal, rheological, mechanical and barrier properties. *Polymer* **2023**, *269*, 125712. [CrossRef]
14. Walha, F.; Lamnawar, K.; Maazouz, A.; Jaziri, M. Biosourced blends based on poly (lactic acid) and polyamide 11: Structure–properties relationships and enhancement of film blowing processability. *Adv. Polym. Technol.* **2018**, *37*, 2061–2074. [CrossRef]
15. Cheng, J.; Qian, Z.; Li, Z. A cumulative fatigue damage model of polysilicon films for MEMS resonator under repeated loadings. *Int. J. Fatigue* **2021**, *147*, 106186. [CrossRef]
16. Zhang, L.H.; Shang, D.-G.; Liu, X.D.; Sun, Y.J.; Guo, Y.B.; Liu, F.Z.; Chen, T. A nonlinear fatigue damage-healing model for copper film by LSP. *Fatigue Fract. Eng. Mater. Struct.* **2014**, *37*, 1232–1241. [CrossRef]

17. Benavides, E. General Model for Reliability-Based Engineering Design. *Commun. Stat. Theory Methods* **2014**, *43*, 2342–2356. [CrossRef]
18. Tiwana, A.; Reddy, C. Life Estimation of LDPE Film under Stepped-Stress Voltage Application. In Proceedings of the IEEE Conference on Electrical Insulation and Dielectric Phenomena (IEEE CEIDP), Toronto, ON, Canada, 16–19 October 2016; pp. 927–930.
19. Frangopoulos, T.; Marinopoulou, A.; Goulas, A.; Likotrafiti, E.; Rhoades, J.; Petridis, D.; Kannidou, E.; Stamelos, A.; Theodoridou, M.; Arampatzidou, A.; et al. Optimizing the Functional Properties of Starch-Based Biodegradable Films. *Foods* **2023**, *12*, 2812. [CrossRef]
20. Nelson, W. *Accelerated Testing: Statistical Models, Test Plans, and Data Analyses*; John Wiley & Sons: Hoboken, NJ, USA, 1990.
21. *ASTM D882-10*; Standard Test Method for Tensile Properties of Thin Plastic Sheeting. Plast. (I). ASTM International: West Conshohocken, PA, USA, 2010.
22. Zhu, W.; Deng, Y.; Zhang, Z.; Tan, G.; Guo, X. Effect of tensile stress response for oxide films on the fatigue failure behavior of anodized AA6082 alloys. *Mater. Sci. Eng.* **2022**, *850*, 143552. [CrossRef]
23. Liu, B.; Chen, K.; Zhou, R. Damage evolution and fatigue life prediction of the shape memory alloy under low cycle fatigue. *Mater. Today Commun.* **2021**, *26*, 101636. [CrossRef]
24. Zuo, M.; Song, Y.; Zheng, Q. Influence of equibiaxial extensional strain on stress relaxation of glycerol plasticised wheat gluten. *J. Sci. Food Agric.* **2008**, *88*, 2350–2356. [CrossRef]
25. McCann, T.H.; Homer, S.H.; Øiseth, S.K.; Day, L.; Newberry, M.; Regina, A.; Lundin, L. High amylose wheat starch increases the resistance to deformation of wheat flour dough. *J. Cereal Sci.* **2018**, *79*, 440–448. [CrossRef]
26. Ranathunga, A.; Suwannaporn, P.; Kiatponglarp, W.; Wansuksri, R.; Sagis, L.M.C. Molecular structure and linear-non linear rheology relation of rice starch during milky, dough, and mature stages. *Carbohydr. Polym.* **2023**, *312*, 120812. [CrossRef]
27. Zullo, R.; Iannace, S. The effects of different starch sources and plasticizers on film blowing of thermoplastic starch: Correlation among process, elongational properties and macromolecular structure. *Carbohydr. Polym.* **2009**, *77*, 376–383. [CrossRef]
28. Liu, Z.; Chen, L.; Zheng, B. New insights into the effects of starch-oleic acid-chlorogenic acid interactions on structural formation by hot-extrusion 3D printing: From perspective of nonlinear rheology. *Food Hydrocol.* **2023**, *144*, 109024. [CrossRef]
29. Bagdahn, J.; Sharpe, W.N.; Jadaan, O. Fracture strength of polysilicon at stress concentrations. *J. Microelectromechanical Syst.* **2003**, *12*, 302–312. [CrossRef]
30. Hedayati, R.; Alavi, M.; Sadighi, M. Effect of Degradation of Polylactic Acid (PLA) on Dynamic Mechanical Response of 3D Printed Lattice Structures. *Materials* **2024**, *17*, 3674. [CrossRef] [PubMed]
31. Averett, R.D.; Realff, M.L.; Jacob, K.; Cakmak, M.; Yalcin, B. The mechanical behavior of poly(lactic acid) unreinforced and nanocomposite films subjected to monotonic and fatigue loading conditions. *J. Compos. Mater.* **2011**, *45*, 2717–2726. [CrossRef]
32. Deshoulles, Q.; Gall, M.L.; Benali, S.; Raquez, J.M.; Dreanno, C.; Arhant, M.; Priour, D.; Cerantola, S.; Stoclet, G.; Gac, P.Y.L. Hydrolytic degradation of biodegradable poly(butylene adipate-co-terephthalate) (PBAT)—Towards an understanding of microplastics fragmentation. *Polym. Degrad. Stab.* **2022**, *205*, 110122. [CrossRef]
33. Kianifar, M.; Azadi, M.; Heidari, F. Evaluation of stress-controlled high-cycle fatigue characteristics in PLA-wood fused deposition modeling 3D-printed parts under bending loads. *PLoS ONE* **2024**, *19*, e0300569. [CrossRef]
34. Kim, W.-G.; Park, J.-Y.; Ekaputra, I.M.W.; Kim, S.-J.; Jang, J. Influence of Hold Time and Stress Ratio on Cyclic Creep Properties Under Controlled Tension Loading Cycles of Grade 91 Steel. *Nucl. Eng. Technol.* **2017**, *49*, 581–591. [CrossRef]
35. Lv, Y.; Huang, Y.; Kong, M.; Yang, J.; Yang, Q.; Li, G. Creep lifetime prediction of polypropylene/clay nanocomposites based on a critical failure strain criterion. *Compos. Sci. Technol.* **2014**, *96*, 71–79. [CrossRef]

Disclaimer/Publisher's Note: The statements, opinions and data contained in all publications are solely those of the individual author(s) and contributor(s) and not of MDPI and/or the editor(s). MDPI and/or the editor(s) disclaim responsibility for any injury to people or property resulting from any ideas, methods, instructions or products referred to in the content.